Chemical Engineering Journal 338 (2018) 636–650

Contents lists available at ScienceDirect

Chemical Engineering Journal

journal homepage: www.elsevier.com/locate/cej

Hydrodynamics of countercurrent bubble column: Experiments and predictions

R. Trivedi, T. Renganathan*, K. Krishnaiah[1]

Department of Chemical Engineering, Indian Institute of Technology Madras, Chennai 600 036, India

HIGHLIGHTS

- Study of hydrodynamics of countercurrent bubble column with a porous distributor.
- Comprehensive flow regime map developed with all four regimes.
- Method developed to predict gas holdup and transition gas velocity semi-empirically.
- Estimated bubble diameter decreases with liquid velocity in homogeneous regime.
- Apparent slip velocity increases with phase velocities in heterogeneous regime.

GRAPHICAL ABSTRACT

Prediction of gas holdup and regime transition points combining two phenomenological models.

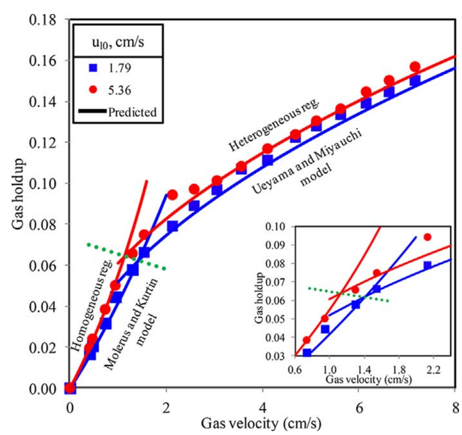

ARTICLE INFO

Keywords:
Bubble column
Countercurrent
Hydrodynamics
Flow regimes
Gas holdup
Apparent slip velocity

ABSTRACT

Experiments were conducted to study the hydrodynamics of a countercurrent bubble column equipped with porous plate distributor. Four flow regimes – purely homogeneous bubbling regime, discrete bubbling regime, helical flow regime and churn-turbulent regime are identified based on the bubble swarm velocity plot. Regime maps are presented showing the effect of liquid velocity on transition gas velocity and gas holdup along all three transition boundaries. The liquid velocity advances the onset of discrete bubbling regime, helical flow regime and churn-turbulent regime. Gas holdup increases with an increase in gas and liquid velocities. A methodology for predicting the gas holdup for both the homogeneous and heterogeneous regimes and the transition gas velocity and holdup is developed by extending existing models for homogeneous and heterogeneous regime. Bubble diameter, the model parameter in homogeneous regime, decreases with an increase in liquid velocity. Apparent slip velocity between gas and liquid phase, the model parameter in heterogeneous regime, increases with both gas and liquid velocity. The method predicts the data of the present work and literature satisfactorily. The effect of gas and liquid velocities on the radial profile of liquid velocity and its properties are simulated using the validated model.

* Corresponding author.
E-mail address: renga@iitm.ac.in (T. Renganathan).
[1] Present address: Indian Institute of Technology Tirupati, Tirupati 517 506, India.

https://doi.org/10.1016/j.cej.2018.01.023
Received 9 August 2017; Received in revised form 3 January 2018; Accepted 4 January 2018
Available online 05 January 2018
1385-8947/

Nomenclature

A, B, C	Parameters in the apparent slip velocity correlation Eq. (35)
c	Parameter in Eq. (15)
d_b	diameter of bubble, m
D	diameter of column, m
Fr_g	Gas phase Froude number, dimensionless
g	acceleration due to gravity, m/s^2
H	Height of the column, m
h	pressure head of water, m
$I(\phi)$	Eq. (26)
J_0, J_1	Eqs. (24) and (25)
Mo_l	Liquid phase Morton number, dimensionless
n	Exponent in Eq. (15)
P	Pressure, Pa
$\Delta P/\Delta z$	Pressure gradient
R	Radius of the column, m
r	Radial coordinate, m
r_o/δ	Length ratio, Eq. (2)
Re	Bubble Reynolds number, dimensionless
Re_g	Gas phase Reynolds number, dimensionless
u_{g0},u_{l0}	Superficial phase velocities = $\frac{Volumetric\ flow\ rate}{Column\ cross-sectional\ area}$
u_g,u_l	Interstitial phase velocities, m/s
u_{lc}	Centreline velocity of liquid, m/s
u_{lw}	Liquid velocity at wall, m/s
$u_{l\delta}$	u_l at y = δ, m/s (Eq. (9))
u_s	Apparent slip velocity of bubbles, m/s
$u_{l_{rec}}$	Mean liquid recirculation velocity, m/s
z	Axial coordinate, m

Greek letter

β	Dimensionless bubble diameter, dimensionless
β_0	Dimensionless bubble diameter at batch liquid condition, dimensionless
δ	Thickness of the laminar sublayer, m
ε_c	Centreline gas holdup, dimensionless
ε_g	Average gas holdup, dimensionless
ε_{gr}	Radial gas holdup, dimensionless
ν_t	Turbulent kinematic viscosity, m^2/s
ν	Molecular kinematic viscosity, m^2/s
ρ_l,ρ_g	Phase density, kg/m^3 ξ
τ	Shear stress, kg/ms^2
τ_w	Shear stress at wall, kg/ms^2
ϕ	r/R, Radial coordinate, dimensionless
ϕ^*	Radial coordinate at which flow reverses, dimensionless
μ_g,μ_l	Phase viscosity, kg/m.s
ζ	Dimensionless parameter, Eq. (2)

Abbreviation

AR	Aspect Ratio
CCBC	Continuous Countercurrent Bubble Column
RMS	Root Mean Square

Subscript

g	gas
l	liquid
Exp	Experimental
Pred	Predicted

1. Introduction

Bubble columns in which gas is sparged into a batch of liquid have high heat and mass transfer characteristics and are easy to operate, as there are no moving parts. These multiphase contactors find applications in chemical, biochemical and metallurgical industries [1]. Bubble columns, used for applications such as hydrogenation, fermentation usually have the liquid phase in batch mode. However, applications such as waste-water treatment and ozonation of water involve continuous flow of the liquid phase [2]. Countercurrent flow of liquid has the advantage of high holdup leading to higher mass transport rates [1]. Countercurrent flow of gas and liquid also occurs in three-phase inverse fluidized bed which can be considered as a countercurrent bubble column (CCBC) with suspended solids [3,4].

Experimental studies on bubble column have predominantly been carried out with the liquid phase under batch condition. Relatively few studies have been carried out with continuous flow of liquid. Among these studies with continuous liquid phase flow, fewer studies have been reported on countercurrent flow compared to cocurrent flow bubble columns. A summary of hydrodynamic studies conducted is presented in Table 1. It can be observed that except for the recent comprehensive studies by Besagni and Inzoli [5] and Besagni et al. [6],

Table 1
Summary of literature on hydrodynamics of CCBC.

Authors	D; H; AR (m)	Gas sparger	u_{g0} (cm/s)	u_{l0} (cm/s)	Hydrodynamic aspects studied		
					Flow regimes	Gas holdup	Bubble size distribution
Eissa and Schügerl [31]	0.159; 3.9; 24.5	Perforated plate	0–6	0.35, 0.7, 1.05	✗	✓	✗
Todt et al. [52]	0.14; 3.8; 27.1	Perforated plate	0.67–10.67	0.7–2.38	✗	✓	✗
Otake et al. [7]	0.05; 1.5; 30	Single and multi-nozzles	0.7–8.24	0–14	✗	✓	✗
Uchida et al. [8]; Seno et al. [9]	0.046; 1.36; 29.5	Single nozzle and porous glass ball filter	0–4	0–10	✓	✓	✗
Ityokumbul et al. [22]	0.06; 1.06; 17.7	Porous plate	0–4	0–0.76	✓	✓	✗
Roustan et al. [10]	0.15; 2.5; 16.7	Porous distributor	0.19–2.08	0.44–2.08	✗	✓	✓
Hidaka et al. [11]	0.07; 4.25; 60.7 & 0.15; 2.6; 18	Spiral copper tube	2–30	0–15	✗	✓	✗
Bin et al. [15]	0.15; 5.5; 36.7	Porous gas distributor	0.47–1.88	0.16–0.71	✗	✓	✗
Son et al. [16]	0.152; 3.5; 23	Pipe distributor	1–3.5	0–3	✗	✓	✓
Jin et al. [12]	0.16; 2.5; 15.6	Perforated plate	2–25	0–1.12	✓	✓	✗
Shah et al. [14]	0.29; 2; 6.9	Perforated plate	2–11	0.05–0.2	✗	✓	✗
Hernandez-Alvarado et al. [13]	0.1; 1.6; 16	Not available	4.6–20.6	2.1–20	✗	✓	✗
Besagni & Inzoli [5]; Besagni et al. [6]	0.24; 5.3; 22.1	Spider sparger	0.4–20	0–9.2	✓	✓	✓